# REVIEW OF THE TRAJECTORY AND ATMOSPHERIC STRUCTURE RECONSTRUCTION FOR MARS PATHFINDER

**Paul Withers**(1), **Martin Towner**(2), **Brijen Hathi**(2), **John Zarnecki**(2)

(1) *Center for Space Physics, Boston University, 725 Commonwealth Avenue, Boston, MA 02215, USA (email: withers@bu.edu)*
(2) *Planetary and Space Science Research Institute, Open University, Walton Hall, Milton Keynes, MK7 6AA, Great Britain*

## ABSTRACT

Mars Pathfinder landed on Mars on July 4, 1997. It used a novel deceleration procedure, consisting of a hypersonic aeroshell, a transonic parachute, retrorockets, and airbags, to reach the surface safely. Its aerodynamic properties passively maintained a near-zero angle of attack throughout its entry. There were no gyroscopes to monitor attitude. Several different trajectory reconstructions have been based on the assumptions that accelerations along its symmetry axis are directed along its flight path and that accelerations in other directions are insignificant. The aerodynamics of Pathfinder once its parachute opened are still not well-understood and the available observations are probably not sufficient to improve matters significantly in the future.

## 1 INTRODUCTION

The aims of this paper are to describe the entry, descent, and landing of Mars Pathfinder (MPF) and to describe the work done to reconstruct its trajectory and atmospheric structure after flight. The current authors were not involved in the Pathfinder mission, so did not perform any of the work described here. We became familiar with this work through our ongoing efforts related to the entry of Beagle 2 into the martian atmosphere, since Pathfinder provided an invaluable test case for the development of our Beagle 2 analysis tools.

"The Mars Pathfinder was the second of NASA's low-cost planetary Discovery missions. It has the primary objective of demonstrating the feasibility of low-cost landings on and exploration of the Martian surface" [15]. Pathfinder was launched from Cape Canaveral, Florida, USA, on a Delta II launch vehicle on 4 December, 1996.

"Mars Pathfinder (named the Sagan Memorial Station) landed on the surface of Mars on 4 July 1997, deployed a small rover (named Sojourner), and collected data from three scientific instruments [named Imager for Mars Pathfinder (IMP), alpha-proton x-ray spectrometer (APXS), and atmospheric structure investigation/meteorology package (ASI/MET)] and technology experiments. In the first month of surface operations the mission returned about 1.2 gigabits of data, which include 9669 lander and 384 rover images and about 4 million temperature, pressure, and wind measurements. The rover traversed a total of about 52 m in 114 commanded movements, performed 10 chemical analyses of rocks and soil, carried out soil mechanics and technology experiments, and explored over 100 m$^2$ of the martian surface" [8].

The scientific results of Pathfinder are published in special issues of Science and Journal of Geophysical Research - Planets [8, 9, 10]. A special issue of Journal of Spacecraft and Rockets on aeroassist systems includes many articles on the engineering challenges of Mars Pathfinder [3].

Fig. 1, taken on the surface of Mars, shows the Sojourner rover, which is parked on one of the three solar panels, ready to drive onto the martian surface. Deflated airbags can be seen at the edges of the solar panel. Fig. 2, taken by the Sojourner rover, shows the squat Pathfinder lander above its deflated airbags, with the IMP deployed above the lander.

## 2 PATHFINDER'S ENTRY, DESCENT, AND LANDING

Fig. 3 shows the spacecraft on Earth during the final stages of testing. An exploded schematic view is shown in Fig. 4. The cruise stage, which provided power and thrust during the journey from Earth to Mars, sits above the aeroshell. The aeroshell consists of a conical backshell and a more rounded front heatshield. A parachute was packed in the point of the backshell and three retrorockets were mounted inside the backshell. The actual lander, with its solar panels folded to form a tetrahedron, sat between the backshell and the heat shield. The lander on Earth is shown in Fig. 5 just prior to folding the last solar

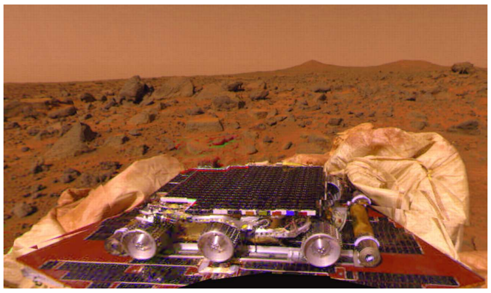

Figure 1: Sojourner rover about to leave the Pathfinder lander. Golombek et al. (1997) Science, 278, 1743-1748.

Figure 2: The Pathfinder lander as seen from the Sojourner rover. http://photojournal.jpl.nasa.gov/-catalog/PIA01121/

panel up.

Pathfinder's entry, descent, and landing (EDL) are summarized in Figs. 6 and 7. Pathfinder entered the atmosphere directly from interplanetary cruise, unlike the Viking landers that were released from an orbiter. A comparison of Pathfinder and Viking's atmospheric entries is shown in Fig. 8. Direct entry led to a high entry speed of 7 km $s^{-1}$, about Mach 40, for Pathfinder. At about 130 km altitude, it had an initial flight path angle of 14 degrees below the horizontal (in the reference frame of Spencer et al.


Figure 3: Pathfinder's cruise stage (top) and aeroshell (bottom) prior to launch. http://mars.jpl.nasa.gov/MPF/nasa/figstabs/-figures/

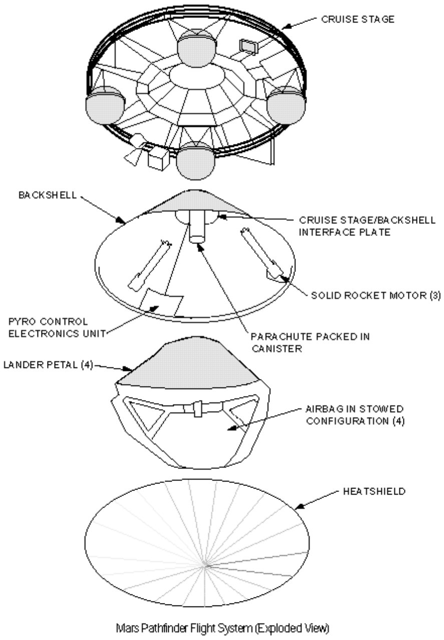


Figure 4: Exploded view of Mars Pathfinder flight system. http://atmos.nmsu.edu/PDS/data/-mpam_0001/document/images/insthst2.gif

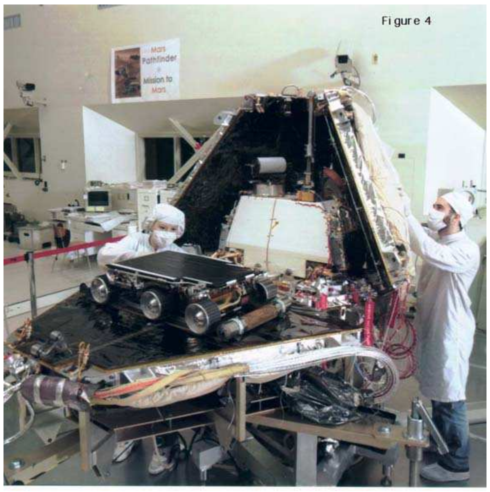


Figure 5: Pathfinder lander, with Sojourner rover attached, prior to folding up the last solar panel. http://mars.jpl.nasa.gov/MPF/nasa/-figstabs/figures/

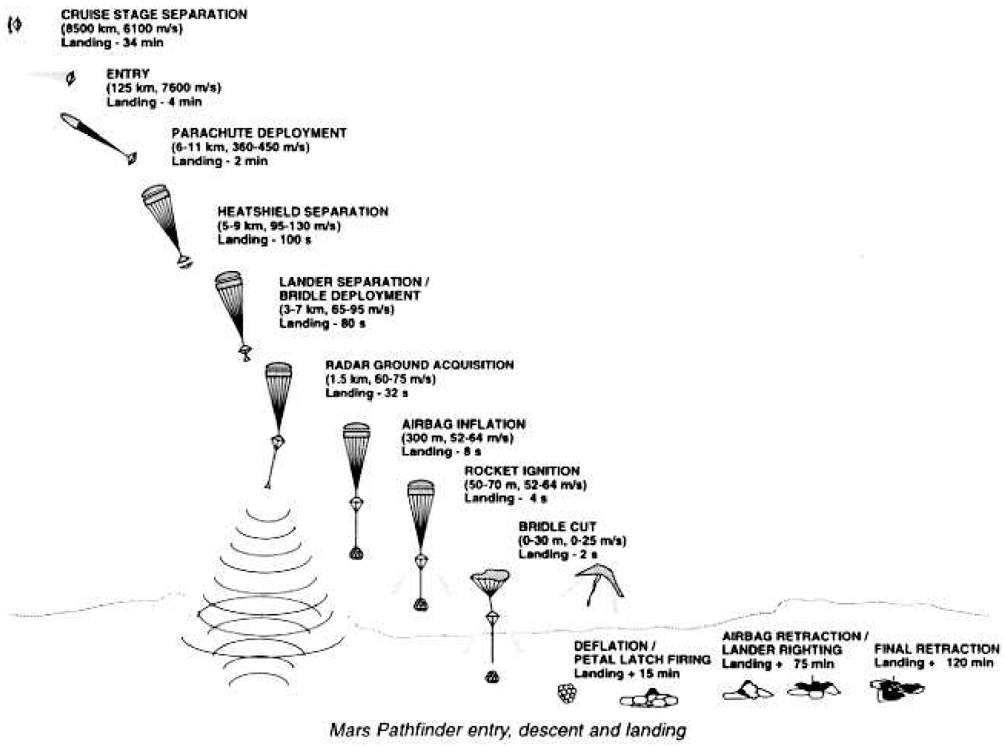


Figure 6: Cartoon of major events during Pathfinder's EDL. http://atmos.nmsu.edu/PDS/data/mpam_0001/-document/images/edler_ds.tif

[19]), so the vertical component of its velocity was about 2 km $s^{-1}$. The entry latitude and longitude were 23$^o$N and 338$^o$E, and the local solar time was 0300 hrs. This time of day ensured slow horizontal winds and small vertical wind shear, unlike the MER entries.

Pathfinder had a near-zero angle of attack between its symmetry axis and the direction of its velocity relative to the atmosphere. It was spinning about its symmetry axis at a roll rate of 2 revolutions per minute upon entry. There was no active attitude control nor guidance; instead, the aerodynamics of the aeroshell were relied upon to passively maintain the angle of attack within a few degrees of zero. With a near-zero angle of attack, unlike Viking's actively maintained 11 degree angle of attack, Pathfinder's entry was effectively free of lift or side forces. The spacecraft's spin was designed to be fast enough that the inevitable lift and side forces, which occurred when the angle of attack was not precisely zero, were averaged to near-zero by the continual change of direction. The spacecraft's spin was designed to be slow enough that its attitude in an inertial frame could change to track changes in flight path angle during EDL. A rapid spin rate, and subsequent gyroscopic stiffness, would have caused an undesirable

| Event | Time | Altitude | Velocity |
|---|---|---|---|
| Cruise stage separation | L - 35 min | | |
| Entry | L - 5 min | 130 km | 7470 m/s |
| Parachute deployment | L - 134 s | 9.4 km | 370 m/s, 16$g$ |
| Heatshield separation | L - 114 s | | |
| Lander separation | L - 94 s | | |
| Radar ground acquisition | L - 28.7 s | 1.6 km | 68 m/s |
| Airbag inflation | L - 10.1 s | 355 m | |
| Rocket ignition | L - 6.1 s | 98 m | 61.2 m/s |
| Bridle cut | L - 3.8 s | 21.5 m | |
| Landing | 2:58 a.m. | 0 | 14 m/s, 19$g$ |
| Roll stop | L + 2 min | | |
| Deflation | L + 20 min | | |
| Airbag retracted | L + 74 min | | |
| Petals opened | L + 87 min | | |

Figure 7: Timeline of major events during Pathfinder's EDL. Golombek et al. (1997) Science, 278, 1743-1748.

**Table 1 Mars Pathfinder and Viking entry comparison**

| Entry characteristic | Mars Pathfinder | Viking |
|---|---|---|
| $V_{e,\text{inertial}}$, km/s | 7.4[a] | 4.73[a], 4.65[b] |
| $V_{e,\text{relative}}$, km/s | 7.6 (retrograde) | 4.50[a], 4.42[b] (direct) |
| $\gamma_{e,\text{relative}}$, deg | −14.8[a] | −17.63[b] |
| Entry mass, kg | 552.0 | 980.8 |
| $S$, m$^2$ | 5.52 | 9.62 |
| $\alpha$, deg | 0.0 | −11.1 |
| $C_D$ | 1.7 | 1.6 |
| Ballistic coefficient, kg/m$^2$ | 58.8 | 63.7 |
| $L/D$ | 0.0 | 0.18 |
| Guidance and control system | Spin stabilized | Three-axis control |

[a]Measured at 125-km altitude. [b]Measured at 243.8-km altitude.

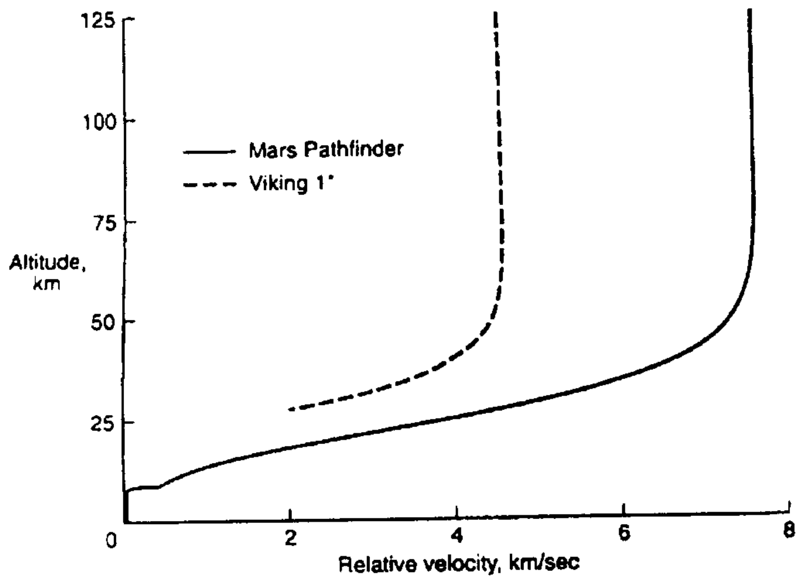


**Fig. 2 Mars Pathfinder and Viking entry profile comparison.**

Figure 8: Comparison of Pathfinder and Viking's atmospheric entries. Braun et al. (1995) J. Spacecraft and Rockets, 32(6), 993-1000

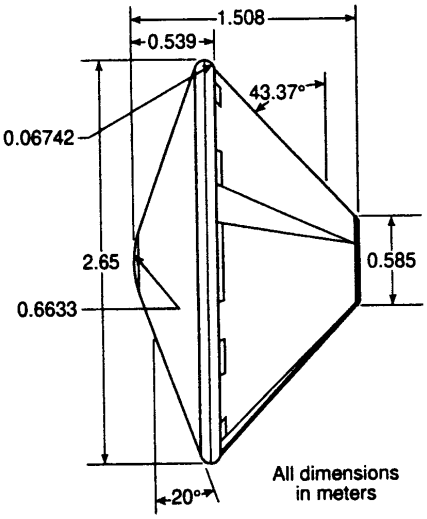


Figure 9: Pathfinder aeroshell dimensions. Spencer et al. (1999) J. Spacecraft and Rockets, 36(3), 357-366

increase in the angle of attack. Spinning also helped to damp the angle of attack towards zero [2].

The 2.65 m diameter aeroshell is a Viking-heritage 70 degree half-angle sphere-cone, scaled down in size from Viking. Pathfinder's entry mass was 585.3 kg and its reference frontal area was 5.536 $m^2$. Its shape is axisymmetric about its z-axis and the centre of mass is on the symmetry axis. It is shown in Fig. 9. The forebody heatshield was coated with a 2 cm layer of an ablative material, SLA-561V. The backshell received a thin, spray-on coating of the same material [18]. Its speed did not change significantly until about 60 km altitude and peak deceleration of 15 g occurred at about 30 km altitude.

At 9 km altitude and 380 m $s^{-1}$ (Mach 1.8), a mortar was fired to deploy the Viking-heritage 12.7 m diameter disk-gap-band parachute on suspension lines longer than 20 m. The parachute was attached to the top of the backshell. Shortly afterwards, the front heatshield was released and fell away. Next, a 20 m long Kevlar bridle was unwound to suspend the tetrahedral lander below the backshell. The aerodynamics of this parachute-backshell-lander system were complicated, and the centre of mass moved from the position that it occupied during the hypersonic entry. At 1.5 km altitude, a radar altimeter began to measure the altitude and descent speed of the lander. At 300 m altitude, four sets of six airbags (one for each side of the tetrahedral lander) were inflated in 0.5 seconds to enclose the lander. Images of the airbags from testing are shown in Figs. 10 and 11.

At 100 m altitude, the three solid fuel retrorockets

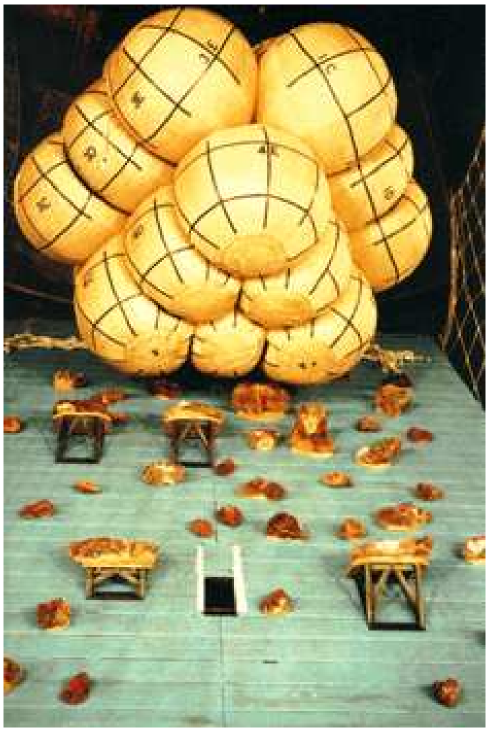

Figure 10: Pathfinder airbags being dropped onto a rocky and inclined plane to simulate landing on Mars. http://mars3.jpl.nasa.gov/MPF/mpf/-mpfairbags.html

Figure 11: Airbags being prepared for testing, with person for scale. http://mars3.jpl.nasa.gov/MPF/-mpf/mpfairbags.html

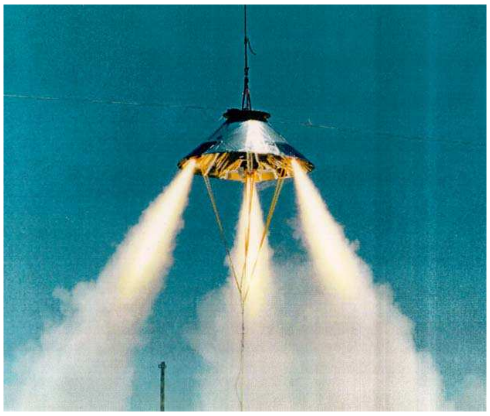

Figure 12: Test firing of Pathfinder's retrorockets. http://mars3.jpl.nasa.gov/MPF/mpf/rad.html


Figure 13: Artist's rendition of lander separating from backshell. http://mars.jpl.nasa.gov/MPF/-rovercom/images/concept-edl.jpg

mounted on the backshell ignited. Each was 85 cm long and 13 cm wide, and generated 8000 N of thrust for 2.2 seconds. A terrestrial test of these is shown in Fig. 12.

By this time, the lander was 20 m above the ground and had zero descent speed. The bridle joining the lander to the backshell was cut and the last thrust of the retrorockets carried the backshell and parachute away from the lander. Fig. 13 shows an artist's rendition of this event. Images from the lander later showed the backshell and parachute lying together on the ground about 1 km away from the lander. The lander fell the final 20 m, hit the surface with a vertical speed of 12 m s$^{-1}$ and a horizontal speed of 6 m s$^{-1}$, then bounced more than 15 times for longer than 1 minute as it rolled $\sim$1 km away from the impact site. Accelerometer measurements ceased before the lander had stopped rolling, so when it stopped is not known. It came to rest at its final landing site, deflated its airbags, unfurled its solar panels, and waited for sunrise.

The aerodynamic accelerations experienced by Pathfinder during EDL are shown in Fig. 14. A reconstruction of Pathfinder's trajectory during EDL is shown in Fig. 15.

## 3 MEASUREMENTS USEFUL FOR RECONSTRUCTING PATHFINDER'S EDL TRAJECTORY

An initial condition is essential for any trajectory reconstruction and Pathfinder's entry state (position, velocity, and time) was reported at a specified entry interface from tracking of the spacecraft during its cruise. The entry interface was a radial distance from the centre of mass of Mars that is about 200 km above the surface, which is close enough to Mars that only the lowest order terms in the martian gravitational field affect the future trajectory and which is far enough from Mars that the atmosphere has not yet affected the trajectory at all.

During the entry itself, various measurements were made that played a role in the trajectory reconstruction. Onboard accelerometers measured the effects of aerodynamic forces on the spacecraft. The Earth-based antennae of the Deep Space Network measured the Doppler shift in the telemetry signal transmitted by Pathfinder, which gives the line-of-sight speed of Pathfinder. Unfortunately, the transmission frequency was not stable, which makes it difficult to separate shifts in received frequency due to Pathfinder's speed from those due to drift in the transmitter. After the parachute opened and before the airbags inflated, pressure and temperature sensors of the ASI/MET instrument were active. Useful measurements of dynamic pressure were obtained, but the temperature sensors measured only internal spacecraft temperature. The positions of these sensors were not optimal due to engineering trade-offs. Below 1.5 km altitude, a radar altimeter with 0.3 m resolution and 50 Hz sampling rate measured altitude and descent speed. Finally, Pathfinder's landed position was measured with great accuracy by the tracking of its radio signal during many martian days. However, this landed position is about 1 km away from the actual impact position.

Pathfinder carried six accelerometers, all Allied Signal QA-3000-003 single axis units [17]. These work by "electromagnetically restricting a test mass to a precise null position" [11]. These six were divided into two sets of three accelerometers, called science and engineering, with the three accelerometers in each set being mutually orthogonal. The positions and axes of each accelerometer are shown in Fig. 16. Most of the aerodynamic forces during entry were directed along the z, or symmetry, axis due to

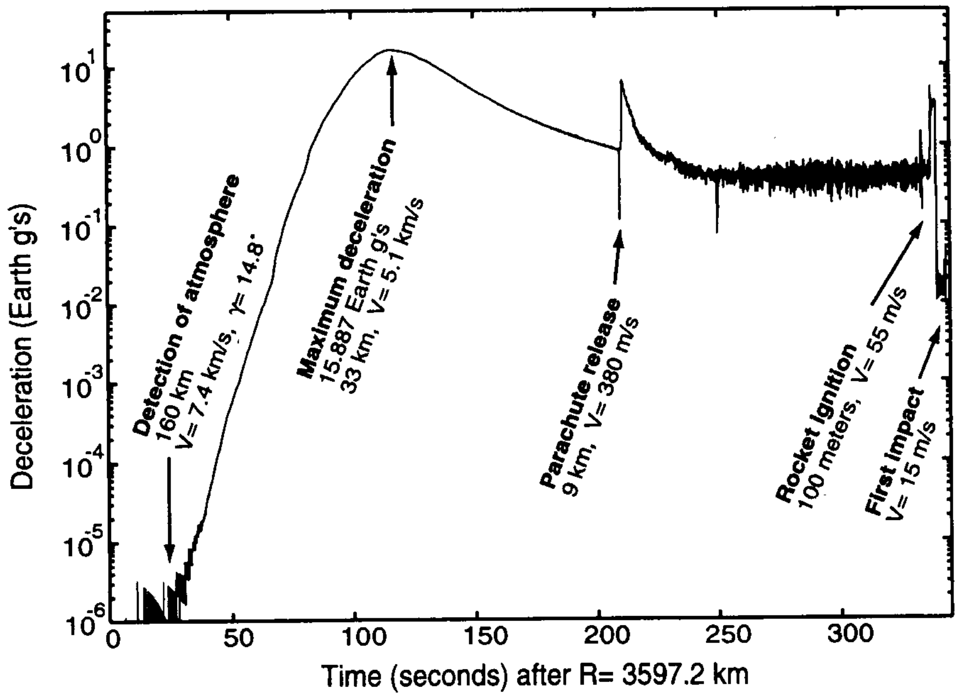


Figure 14: Aerodynamic accelerations experienced by Pathfinder during EDL. Magalhaes et al. (1999) J. Geophys. Res., 104(E4), 8943-8955

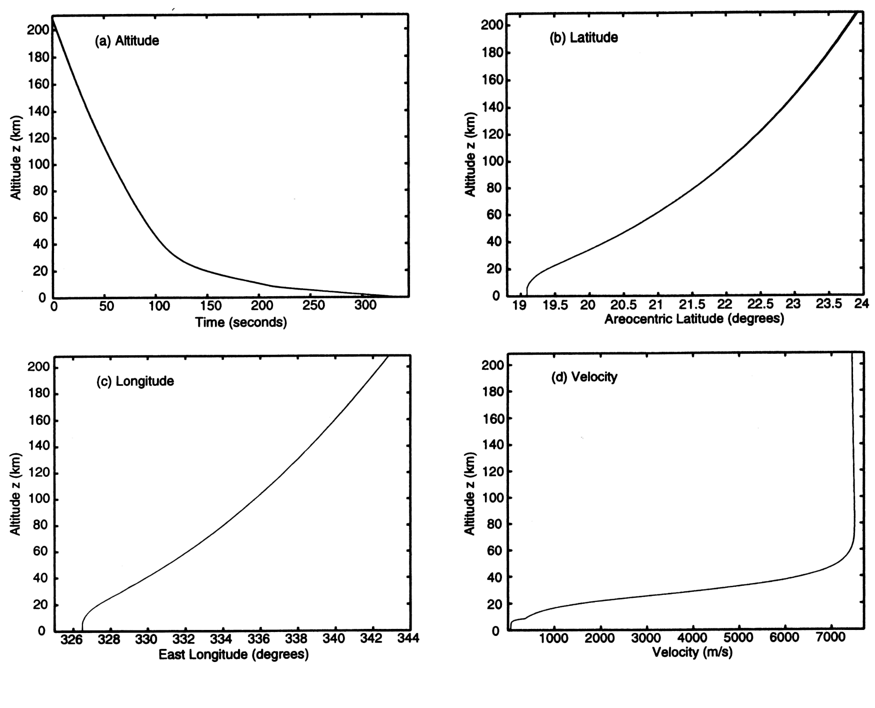


Figure 15: Pathfinder's trajectory during EDL. Magalhaes et al. (1999) J. Geophys. Res., 104(E4), 8943-8955

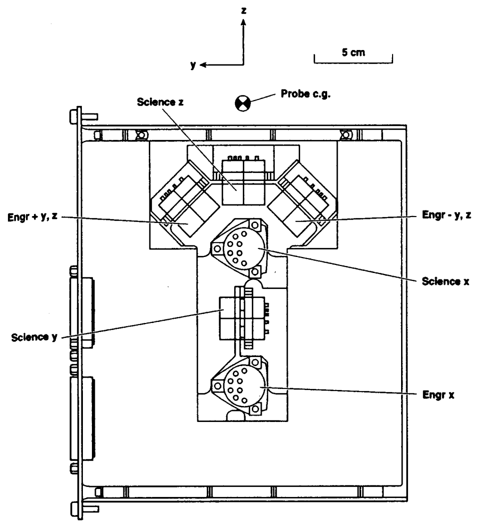


Figure 16: Layout of Pathfinder's six accelerometers. Seiff et al. (1997) J. Geophys. Res., 102(E2), 4045-4056

the near-zero angle of attack. The z-direction science accelerometer is located on the z-axis, about 5 cm away from the centre-of-mass during the hypersonic entry. Recall that the centre-of-mass shifted significantly once the parachute was deployed, which introduced angular accelerations due to rotation about the centre-of-mass into the measured accelerations. The x- and y-direction science accelerometers were located about 10 and 15 cm away, respectively, from the centre-of-mass along the z-axis. Two engineering accelerometers were about 10 cm away from the centre-of-mass in the yz plane, pointing at 45 degrees from the y- and z-axes. The final engineering accelerometer pointed in the x direction and was located the furthest away from the centre of mass. There were no gyroscopes to monitor the spacecraft's orientation, so assumptions and indirect measurements had to be used to constrain this.

The engineering accelerometers were primarily used to trigger the parachute deployment after peak deceleration and to monitor the landing and subsequent bouncing. The science accelerometers were primarily used to measure accelerations during entry as sensitively as possible and to monitor the landing and subsequent bouncing. The engineering accelerometers had one gain state of ± 40 g, whereas the science accelerometers had three gain states, ± 40 g, ± 800 millig, and ± 16 millig. Gain states on the science accelerometers changed to maximize their sensitivity to the current acceleration without going off the scale. With 14 bit digitization, the digitial resolutions of the three gain states were 5 millig, 100 microg, and 2 microg, respectively. The dynamic range of 7 orders of magnitude was superb and was due mainly to the variable gain state of the instruments. With instrument noise levels of 1–2 counts, the z-axis science accelerometer first detected the atmosphere at 160 km altitude and a density of $2\times10^{-11}$ kg m$^{-3}$. Sampling rates on all six accelerometers were 32 Hz.

## 4 VARIOUS TRAJECTORY RECONSTRUCTIONS

The Pathfinder scientists [11] generated one reconstructed trajectory and the Pathfinder engineers [19] generated another two, one simple and one complicated. The scientists' work is also archived in the Planetary Data System (PDS) [16]. The scientists quoted one entry state at about 210 km altitude and the engineers another at about 130 km altitude. These two entry states appear to be inconsistent in that a trajectory extended forwards or backwards in time from one entry state under the influence of gravity does not pass through the other entry state. Also, the entry state quoted by the Pathfinder scientists at 210 km altitude is inconsistent with a figure showing their reconstructed trajectory at about that altitude. All three reconstructed trajectories are consistent with the entry state quoted by the engineers. This problem is discussed further in Withers et al. [20], who concluded that the entry state published by Magalhães et al. [11] and PDS [16] was in error in some way. They further concluded that the entry state published by Magalhães et al. [11] and PDS [16] was not used to generate their published trajectory.

The basic steps common to all trajectory reconstruction processes are as follows. A reference frame is chosen, which may be centred on Mars or elsewhere, which may be inertial or non-inertial, and which may be rotating with Mars or not. The equations of motion appropriate for this frame are written down, eg $dz = v_z dt$, $dv_z = (a_z+g)dt$, etc. An expression for gravitational forces in this frame is derived. Acceleration measurements made in a spacecraft-fixed frame at some position away from its centre of mass are converted to aerodynamic accelerations experienced by the centre of mass in chosen frame. This step is complicated and requires knowledge of the spacecraft orientation in the chosen frame. Starting from the entry state, the equations of motion are integrated forward in time until landing. Additional steps for Pathfinder include worrying about the complicated motion of the parachute-backshell-lander, incorporating the radar altimeter data, and being consistent with the known landed position

The scientists' trajectory reconstruction used a Mars-centred, rotating, spherical coordinate system. Their expression for the martian gravitional field included $J_2$, the first non-spherically symmetric term in the standard spherical harmonic expansion. Magalhães et al. [11] state that the entry state published in that paper was used, with some small changes within the uncertainties to ensure impact at the known landed position, but see above for a discussion of this entry state. They assumed that the accelerations measured by the z-axis scence accelerometer were directed along flight path, giving Pathfinder an angle of attack that was always zero. The x- and y-axis accelerometer data do not appear to have been used. The reconstruction of spacecraft orientation during the parachute descent phase is not discussed explictly, but seems to have followed the same zero angle of attack assumption. The radar altimeter data was used only as an external consistency check.

The engineers' simple trajectory reconstruction used a Mars-centred, non-rotating coordinate system. Their expression for the martian gravational field is not specified. The entry state published in their paper was used initially. They also assumed that the accelerations measured by the z-axis scence accelerometer were directed along flight path, giving Pathfinder an angle of attack that was always zero. The entry state was then adjusted to ensure impact at known landed position <u>and</u> to have best fit to radar altimeter data. Their use of radar data assumed level topography beneath Pathfinder's flight path, which is not a bad assumption.

The engineers' complicated trajectory reconstruction used the same frame and gravitational field as their simple one. An initial trajectory was reconstructed using their best entry state and the z-axis accelerations. A covariance matrix was also obtained, and this reference trajectory was used with the Doppler shift results and the radar altimeter data in a linearized Kalman filter framework to generate an improved trajectory. This technique was then repeated going backwards in time from the landed position, and the two trajectories were combined to produce a single resultant trajectory. The engineers do not say which of their two reconstructions is best.

The three trajectories are basically identical during aeroshell portion of entry. After the parachute opened, differences are found in descent speed ($\sim$10 m s$^{-1}$) and altitude ($\sim$200 m) as a function of time since passing the entry interface. These difference can be attributed to incomplete understanding of Pathfinder's aerodynamics after its parachute opened, different assumptions made concerning those aerodynamics, and different uses of Doppler and radar data to correct those flaws. It is perhaps best to consider the differences between the reconstructions as illustrative of their uncertainties, rather than identifying one as superior to the others. The aerodynamics of the lander/backshell/parachute system are still not perfectly understood. Indeed, the predicted drag coefficient of the parachute was 0.5, whereas it appears to have been closer to 0.4 during flight [4]. Hopefully the 3-axis accelerometer and 3-axis gyroscope on both the backshell and the lander for MER will provide enough information to understand the aerodynamics of such a system fully.

## 5 DATABASE OF PATHFINDER'S AERODYNAMIC COEFFICIENTS

The trajectory reconstruction has thusfar not used any quantitative information about Pathfinder's aerodynamic characteristics at all. Qualitative reasoning has been used to justify the zero angle of attack assumption, but that is all. Of course, the aerodynamic characteristics were used before Pathfinder's EDL to design the nominal trajectory and EDL control algorithms. They are, however, necessary for a reconstruction of the angle-of-attack and atmospheric structure during EDL. In this section, I shall address only the hypersonic entry phase of EDL, prior to parachute deployment, since Pathfinder's aerodynamic characteristics after that point are not well-known.

Given the atmospheric composition, density, and temperature, and spacecraft speed and attitude likely to have been experienced during entry, it is necessary to predict the forces, torques, and heating rates experienced by Pathfinder. These results are provided by the science of aerothermodynamics. They are usually expressed in an aerodynamic database as dimensionless coefficients by normalizing to combinations of characteristic dimensions, such as spacecraft area and mass.

First, a nominal profile of atmospheric composition, density, and temperature as a function of altitude was chosen. Next, a nominal profile of speed as a function of altitude was estimated using the probable entry state and a first-guess aerodynamic database. These environmental conditions are often expressed in terms of the Mach, Reynolds, and Knudsen numbers, Ma, Re, and Kn. About 10–20 points along this nominal trajectory were selected and the corresponding values of atmospheric composition, density, and temperature, and speed were noted. It is important to realize that only one spacecraft speed at any atmospheric density and temperature is considered, so if the eventual trajectory reconstruction suggests that this nominal speed is incorrect, then additional simulations at the correct speed are needed to provide the relevant aerodynamic characteristics.

For $\sim$8 angles of attack, the forces, torques, and heating rates that affect Pathfinder at these points along nominal trajectory were predicted and expressed as dimensionless coefficients. This process was iterated until the input, first-guess aerodynamic database was consistent with the output aerodynamic database.

Wind tunnel tests were not performed to derive Pathfinder's aerodynamic characteristics. Numerical techniques were used instead. However, wind tunnel tests and flight data from Viking were used to validate the computational results for Pathfinder [1]. Two classes of numerical models predicted Pathfinder's aerodynamic characteristics. The first, appropriate to rarefied and transitional flow at the top of the atmosphere where $\mathrm{Kn} > 0.01$, modelled the atmosphere as a collection of individual molecules. The second, appropriate to continuum flow lower in atmosphere where $\mathrm{Kn} < 0.01$, modelled the atmosphere as a continuous fluid.

Rarefied and transitional flow were studied by Moss et al., who used Direct Simulation Monte Carlo models in the G2 and DAC computer codes [12, 13, 14]. In this work, the atmosphere consists of $CO_2$, $N_2$, and their reaction products. These molecules occasionally collide with each other, transferring energy between their rotational and vibrational modes and taking part in chemical reactions. They also hit the spacecraft, after which they rebound in a random direction with a temperature, which sets their speed, equal to the surface temperature of the spacecraft. This transfers momentum and energy to the spacecraft, which gets hotter and slows down. For most of this portion of EDL, Pathfinder's centre of mass is behind its centre of pressure, which causes some instabilities.

Continuum flow was studied by Gnoffo et al. [5, 6, 7]. Their simulations used either a non-viscous, perfect gas in the fast-running HALIS code or a viscous, real gas in the slow-running LAURA code. Most of their simulations used only the forebody part of Pathfinder's shape. The non-viscous simulations incorporated a Rankine-Hugoniot bow-shock with constant enthalpy, flow tangent to the spacecraft's surface at the atmosphere-spacecraft interface, and made some approximations in place of true atmospheric chemical reactions. The viscous simulations have more complicated conditions, including chemical reactions between atmospheric species. Gnoffo et al. predicted two regions of instability during EDL where the angle of attack will steadily increase.

## 6 RECONSTRUCTION OF ATMOSPHERIC STRUCTURE AND ANGLE-OF-ATTACK

The ratio of the drag coefficient, $C_D$, to the lift coefficient, $C_L$, can be simply related to the measured ratio of axial and normal accelerations. At a given speed and atmospheric composition, density, and temperature, this ratio is proportional to the angle of attack. Thus, given the reconstructed trajectory and a preliminary atmospheric structure reconstruction (which needs a preliminary $C_D$), one can use the measured ratio of axial and normal accelerations to determine the angle of attack along the EDL trajectory. This angle of attack can then be used with the preliminary atmospheric structure to determine an improved $C_D$, which can then be used to determine an improved atmospheric structure. This is the basis for an iterative procedure used to find the atmospheric structure, $C_D$, and angle of attack along the EDL trajectory.

The Pathfinder scientists and engineers used essentially identical techniques to reconstruct the atmospheric structure, though the scientists used their reconstructed trajectory and the engineers used their simple reconstructed trajectory. Their results are very similar. Atmospheric density, $\rho$, is related to the aerodynamic drag by Eqn. 1.

$$\rho = \frac{-2m}{C_D A} \times \frac{a_v}{v_R^2} \tag{1}$$

where $m$ is the mass of the spacecraft, $A$ is the reference area of the spacecraft, $C_D$ is the drag coefficient appropriate to the present angle of attack, atmospheric composition, density, and temperature, $a_v$ is the acceleration along the flight path, and $v_R$ is the speed of the spacecraft relative to the atmosphere. This is a pointwise formula that does not involve any integration along the EDL trajectory. However, it does rely on earlier results for atmospheric structure and angle of attack, so this procedure was iterated until convergence was achieved.

Atmospheric pressure, $p$, is related to atmospheric density by the equation of hydrostatic equilibrium, Eqn. 2.

$$p(z) = p(z_0) - \int_{z_0}^{z} \rho g dz \tag{2}$$

This equation is derived from the vertical component of the momentum conservation equation. It neglects the horizontal components of momentum conservation, including any horizontal motion of Pathfinder during EDL. Recall that Pathfinder travelled a few hundred kilometres horizontally during its descent. This is not a major effect, but it is

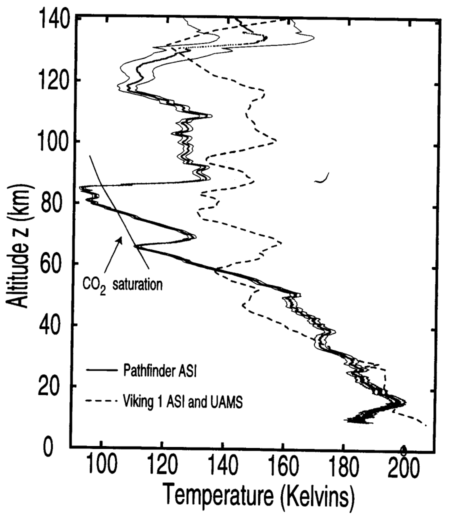


Figure 17: Atmospheric temperature profile measured by Pathfinder. Magalhaes et al. (1999) J. Geophys. Res., 104(E4), 8943-8955

important to be aware of it. Atmospheric entries for which the horizontal winds are known, such as from a Doppler Wind Experiment like Galileo's or Cassini's, might be able to include these effects for a more accurate pressure profile. A boundary condition at the top of the atmosphere is provided by assuming that the atmosphere there is isothermal. The measured density scale height then relates simply to the pressure there. This approximate, but reasonable, boundary condition does not affect pressures more than a few scale heights below this altitude.

Atmospheric temperature, $T$, can be derived from the equation of state for the known atmospheric composition using the ideal gas law, Eqn. 3.

$$T = \frac{m_{mean}}{k_{Boltzmann}} \times \frac{p}{\rho} \tag{3}$$

where $m_{mean}$ is the mean mass of an atmospheric molecule and $k_{Boltzmann}$ is Boltzmann's constant. The derived temperature profile is shown in Fig. 17.

As discussed in the opening paragraph of this section, once this improved atmospheric structure profile is generated, the angle of attack profile can be recalculated and improved, and the appropriate drag coefficient recalculated and improved. This iteration converges quickly, because the drag coefficient changes slowly and no more than linearly with orders of magnitude changes in atmospheric density. The reconstructed angle of attack profile is shown in Fig. 18. The two regions of instability predicted earlier by Gnoffo et al. can be seen around 55 and 85 seconds.

Pathfinder's aerodynamics during the parachute phase of EDL are not known well enough to allow atmospheric structure reconstruction once the parachute has opened at about 9 km altitude.

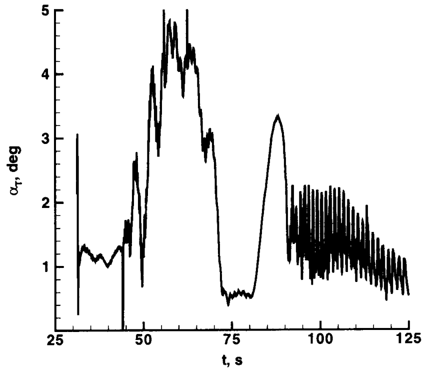


Figure 18: Angle of attack as a function of time since the entry interface. Gnoffo et al. (1998) AIAA 98-2445, http://techreports.larc.nasa.gov/-ltrs/PDF/1998/aiaa/NASA-aiaa-98-2445.pdf

## 7 CONCLUSIONS

Consistency checks are important, because many of the approximations underlying Pathfinder's trajectory reconstruction are based on assumed knowledge of the eventual answers. Do the derived altitudes, latitudes, longitudes, speeds, angle of attacks, densities, pressures, and temperatures agree with all the assumptions that went into the reconstructions? For example, does the angle of attack get large enough to provide lift and invalidate the zero lift assumption? Does a simulated entry of Pathfinder into the reconstructed atmosphere reproduce the same trajectory? Does the nominal trajectory used for generating the aerodynamic database match the observed trajectory? Are deviations from preflight predictions understood? These checks are an essential part of the trajectory reconstruction and have been performed by the Pathfinder scientists and engineers.

Pathfinder's trajectory reconstruction was relatively simple due to its axisymmetry, zero angle of attack with an accelerometer on axis of symmetry close to the centre of mass, the lack of any forces/torques generated by a guidance system, and its entry into an already well-characterized atmosphere. However, measurements during EDL were insufficient to characterize the parachute descent phase accurately. All of the information needed to independently test and verify the published reconstructions is (currently) easily available. These factors make Pathfinder a good test case for developing your own reconstruction tools.

## References


[1] Blanchard R. C., et al. Aerodynamic Flight Measurements and Rarefied-Flow Simulations of Mars Entry Vehicles, *J. Spacecraft and Rockets*, Vol. 34(5), 687-690, 1997.

[2] Braun R. D., et al. Mars Pathfinder Six-Degree-of-Freedom Entry Analysis, *J. Spacecraft and Rockets*, Vol. 32(6), 993-1000, 1995.

[3] Braun R. D. Aeroassist Systems: An Important Element in NASA's New Era of Planetary Exploration, *J. Spacecraft and Rockets*, Vol. 36(3), 297-297, 1999.

[4] Desai P. N., et al. Flight Reconstruction of the Mars Pathfinder Disk-Gap-Band Parachute Drag Coefficient, *17th AIAA Aerodynamic Decelerator Systems Technology Conference and Seminar, May 19-22, Monterey, California, USA*, AIAA-2003-2126, online at http://techreports.larc.nasa.gov/ltrs/PDF/-2003/aiaa/NASA-aiaa-2003-2126.pdf, 2003.

[5] Gnoffo P. A., et al. Effects of Sonic Line Transition on Aerothermodynamics of the Mars Pathfinder Probe, *13th AIAA Applied Aerodynamics Conference, June 19-22, San Diego, California, USA*, AIAA 95-1825, online at http://techreports.larc.nasa.gov/ltrs/PDF/aiaa-95-1825.pdf, 1995.

[6] Gnoffo P. A., et al. Influence of Sonic-Line Location on Mars Pathfinder Probe Aerothermodynamics, *J. Spacecraft and Rockets*, Vol. 33(2), 169-177, 1996.

[7] Gnoffo P. A., et al. Prediction and Validation of Mars Pathfinder Hypersonic Aerodynamic Data Base, *7th AIAA/ASME Joint Thermophysics and Heat Transfer Conference, June 15-18, Albuquerque, New Mexico, USA*, AIAA 98-2445, online at http://techreports.larc.nasa.gov/ltrs/-PDF/1998/aiaa/NASA-aiaa-98-2445.pdf, 1998.

[8] Golombek M., et al. Overview of the Mars Pathfinder mission and assessment of landing site predictions, *Science*, Vol. 278, 1743-1748, 1997.

[9] Golombek, M. Introduction to the special section: Mars Pathfinder, *J. Geophys. Res.*, Vol. 104(E4), 8521-8522, 1999.

[10] Golombek, M. Introduction to the special section: Mars Pathfinder Part 2, *J. Geophys. Res.*, Vol. 105(E1), 1719, 2000.

[11] Magalhães J. A. et al., Results of the Mars Pathfinder atmospheric structure investigation, *J. Geophys Res.*, Vol. 104(E4), 8943-8955, 1999.

[12] Moss J. N., et al. DSMC Simulations of Blunt Body Flows for Mars Entries: Mars Pathfinder and Mars Microprobe Capsules, *32nd AIAA Thermophysics Conference, June 23-25, Atlanta, Georgia*, AIAA Paper 97-2508, online at http://techreports.larc.nasa.gov/ltrs/-PDF/1997/aiaa/NASA-aiaa-97-2508.pdf, 1997.

[13] Moss J. N., et al. Mars Pathfinder Rarefied Aerodynamics: Computations and Measurements, *36th AIAA Aerospace Science Meeting, January 12-15, Reno, Nevada, USA*, AIAA 98-0298, online at http://techreports.larc.nasa.gov/ltrs/-PDF/1998/aiaa/NASA-aiaa-98-0298.pdf, 1998.

[14] Moss J. N., et al. Mars Pathfinder Rarefied Aerodynamics: Computations and Measurements, *J. Spacecraft and Rockets*, Vol. 36(3), 330-339, 1999.

[15] NSSDC — http://nssdc.gsfc.nasa.gov/-planetary/mesur.html

[16] PDS — http://atmos.nmsu.edu/PDS/data/-mpam_0001/

[17] Seiff A, et al. The atmospheric structure and meteorology instrument on the Mars Pathfinder lander, *J. Geophys Res.*, Vol. 102(E2), 4045-4056, 1997.

[18] Spencer D. A., et al. Mars Pathfinder Atmospheric Entry Reconstruction, *AAS/AIAA Space Flight Mechanics Conference, February 9-11, Monterey, California*, AAS 98-146, online at http://techreports.larc.nasa.gov/ltrs/PDF/-1998/mtg/NASA-98-sfmc-das.pdf, 1998.

[19] Spencer D. A., et al. Mars Pathfinder Entry, Descent, and Landing Reconstruction, *J. Spacecraft and Rockets*, Vol. 36(3), 357-366, 1999.

[20] Withers P., et al. Analysis of entry accelerometer data: A case study of Mars Pathfinder, *Planetary and Space Sci.*, Vol. 51, 541-561, 2003.